Phys. Status Solidi A **209**, No. 5, 994–997 (2012) / **DOI** 10.1002/pssa.201127721

physica status solidi a
www.pss-a.com
applications and materials science

Carrier-transport studies of III-nitride/ Si_3N_4/Si isotype heterojunctions

Mahesh Kumar[1,2], Basanta Roul[1,2], Thirumaleshwara N. Bhat[1], Mohana K. Rajpalke[1], A. T. Kalghatgi[2], and S. B. Krupanidhi[*,1]

[1] Materials Research Center, Indian Institute of Science, Bangalore-560012, India
[2] Central Research Laboratory, Bharat Electronics, Bangalore-560013, India

Received 8 December 2011, revised 14 January 2012, accepted 30 January 2012
Published online 6 March 2012

Keywords heterojunctions, MBE, silicon nitrides, transport properties

[*] Corresponding author: e-mail sbk@mrc.iisc.ernet.in, Phone: +91 80 22932943, Fax: +91 80 23607316

GaN/Si_3N_4/n-Si and InN/Si_3N_4/n-Si heterojunctions (HJs) were fabricated using plasma-assisted molecular beam epitaxy for a comparison study. Single-crystalline wurtzite structures of GaN and InN epilayers were confirmed by high-resolution X-ray diffraction and thickness of ultrathin Si_3N_4 layer was measured by transmission electron microscopy. n-GaN/Si_3N_4/n-Si HJs show diode-like rectifying current–voltage (*I–V*) characteristic, while n-InN/Si_3N_4/n-Si HJs show symmetric nonlinear *I–V* behavior. The *I–V* characteristics of both HJs were discussed in terms of the band diagram of HJs and the carrier transport mechanism. The activation energies of carrier conduction were estimated to be ~29 meV for GaN/Si_3N_4/Si and ~95 meV for InN/Si_3N_4/Si HJs.

1 Introduction Semiconducting group-III nitrides have attracted a lot of attention in recent years primarily because of the large gap (0.7–6.2 eV) that can be covered by the nitrides and their alloys. Their optical properties are highly suitable for novel opto-electronic and photonic applications [1–3]. The most attractive property of GaN is its direct wide bandgap (~3.4 eV) and can be alloyed with AlN and InN, which allows tuning of the bandgap from the ultraviolet to the near-infrared region [4, 5]. Silicon is considered to be one of the most promising candidate substrates for GaN and InN epitaxy because of its many advantages such as high quality, large size, low cost, and a well-known existing device technology [6]. However, there exist several hindrances that prevent formation of the high-quality layers. The large mismatch in the lattice parameters of GaN or InN and Si show that the two materials are not particularly compatible. For a direct growth of heterostructures, there is generally a high density of interfacial state between the two materials due to lattice mismatch. The lattice mismatch produces a dislocation field at the junction interface that can attract a space charge and/or act as a recombination center, resulting in degeneration of the device performance. The effective heterointerface allows efficient carrier transport with minimal leakage current. One of the methods of improving the interface quality is to insert a thin interlayer of different materials to passivate defects and change the interface charge. It has been found that growth of a thin silicon nitride interlayer played an important role in improving the GaN and InN layers quality [7–9]. In this work, n-GaN/Si_3N_4/n-Si and n-InN/Si_3N_4/n-Si heterojunctions (HJs) have been fabricated and the current transport properties of these isotype HJs are discussed.

2 Experimental The samples used for this study were grown by a plasma-assisted molecular beam epitaxy (PA-MBE) system equipped with a radio-frequency plasma source. The n-Si (111) substrates were chemically cleaned followed by dipping in 5% HF to remove the surface native oxide. The substrates were thermally cleaned at 900 °C for 1 h in ultrahigh vacuum. The Si_3N_4 layer (~2.5 nm) on Si (111) surface was grown by exposing the surface to RF nitrogen plasma with a high content of nitrogen atoms and details of the growth conditions can be found elsewhere [8]. After nitridation, in sample (a), a low-temperature GaN buffer layer of 20 nm was grown at 500 °C, where the Ga effusion cell temperature was kept at 950 °C and the corresponding beam equivalent pressure (BEP) was maintained at 5.6×10^{-7} mbar. Afterwards, a GaN epilayer of thickness 230 nm was grown on the buffer layer at 700 °C. In sample (b), after nitridation, a low-temperature InN buffer layer of thickness 20 nm was grown at 400 °C followed by 230 nm of InN at 450 °C. The indium effusion cell temperature was kept at 780 °C and the corresponding BEP was maintained at 2.1×10^{-7} mbar. The nitrogen flow rate and plasma power were kept to 0.5 sccm and 350 W, respectively, for the nitridation, buffer layer, and subsequent growth. The structural evaluation of epilayers was carried out by high-resolution X-ray diffraction (HRXRD), and transmission electron microscopy (TEM) was employed to examine the interface of the HJs. The aluminum circular contacts of diameter 400 μm were fabricated by thermal evaporation using a physical mask. The adequate ohmic nature of the contacts to InN, GaN, and Si was verified. The variable-temperature characteristics of the devices were measured using a Keithley-236 source measure unit.

3. Results and discussion Figure 1a and b shows the HRXRD 2θ–ω scans of GaN and InN epilayers grown on the Si (111) substrate. In sample (a), a strong (0002) GaN diffracted peak at $2\theta = 34.59°$ and a weak (0004) GaN peak at $2\theta = 73°$ and in sample (b), a strong (0002) InN diffracted peak at $2\theta = 31.32°$ and a weak (0004) InN peak at $2\theta = 65.32°$ are observed, in addition to the substrate peaks. These diffraction results establishing the epitaxial nature of GaN and InN thin-film highly oriented along the [0001] direction of the hexagonal wurtzite structure. For evaluating the interface features between the GaN layers and Si substrates, lattice images were taken by using cross-sectional TEM. Figure 1c and d shows the cross-sectional transmission electron micrographs and high-resolution TEM (HRTEM) image of GaN/Si_3N_4/Si HJs. In the TEM images, a well-defined Si_3N_4 layer with thickness of ~2.5 nm was observed on the Si surface. The carrier densities of Si, GaN, and InN were measured by Hall measurements. The Si, GaN, and InN

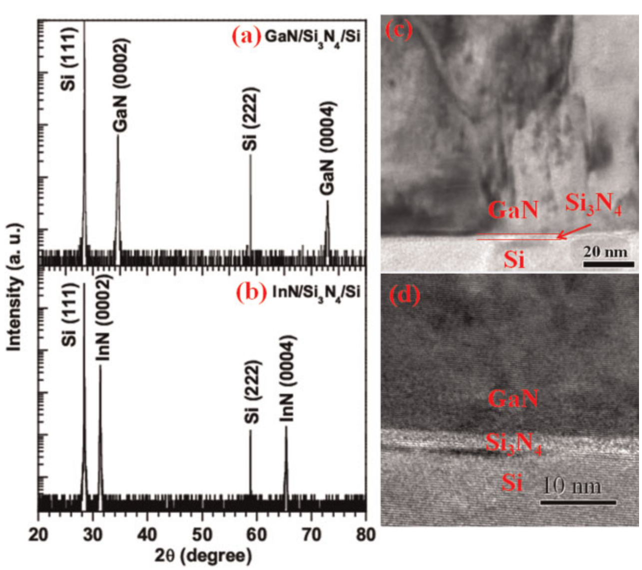

Figure 1 (online color at: www.pss-a.com) HRXRD 2θ–ω scans of (a) GaN and (b) InN epilayers on Si (111). (c) and (d) Cross-section TEM and HRTEM images of GaN/Si_3N_4/Si HJs, respectively.

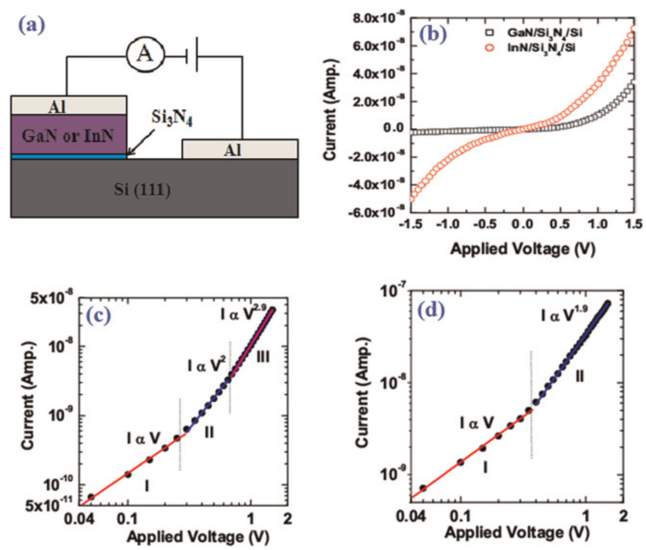

Figure 2 (online color at: www.pss-a.com) (a) Schematic diagram of device and (b) the I–V characteristics of the GaN/Si_3N_4/Si and InN/Si_3N_4/Si HJs measured at room temperature. (c) and (d) Log-log plots of the I–V under forward bias of GaN/Si_3N_4/Si and InN/Si_3N_4/Si HJs, respectively.

exhibit n-type conduction, with electron concentration of $\sim 2 \times 10^{17}$, $\sim 6 \times 10^{17}$, and 5×10^{19} cm^{-3}, respectively.

A schematic diagram of HJs is shown in Fig. 2a and b exhibits the I–V plot of the device measured at room temperature. The n-GaN/Si_3N_4/n-Si HJs show good rectifying behavior with an on/off ratio (I_F/I_R at 1.5 V) of 16, while n-InN/Si_3N_4/n-Si HJs show relatively poorer rectifying behavior with an on/off ratio (I_F/I_R at 1.5 V) of 1.5. In sample (a), the reverse leakage current is found to be 2.4×10^{-9} A at 1.5 V, while in sample (b) it was 5×10^{-8} A at 1.5 V. The possible transport mechanism responsible in these HJs is discussed in the following. The energy-band diagrams of both types of HJs at equilibrium and under bias that are derived from the Anderson model are shown in Fig. 3. The electron affinities of GaN, InN, Si_3N_4, and Si were taken as 3.1, 5.8, 2.1, and 4.05 eV, respectively [10, 11], while the bandgaps of GaN, InN, Si_3N_4, and Si were taken as 3.42, 0.7, 5.3, and 1.1 eV, respectively. For n-GaN/Si_3N_4/n-Si HJs, the bands of Si near the Si/Si_3N_4 interface will bend upward with a positive bias applied on the Si (Fig. 3a and b). It can be seen from Fig. 3b that, under the influence of the electric field, electrons could tunnel through the barrier and drift toward the Si side driven by the applied bias. While, when the junction is negatively biased (a negative bias is applied on the Si side), electrons are confined in the Si side because of the large conduction band offset and resulted in much less leakage current. The InN epilayers were unintentionally doped, which shows n^+-type conductivity and the Fermi level lies in the conduction band (Fig. 3c and d). For n-InN/Si_3N_4/n-Si HJs, the electron will tunnel through the Si_3N_4 barrier layer in the forward- and reverse-bias conditions. The conduction-band offset is not an effective barrier in this case because the InN is highly doped

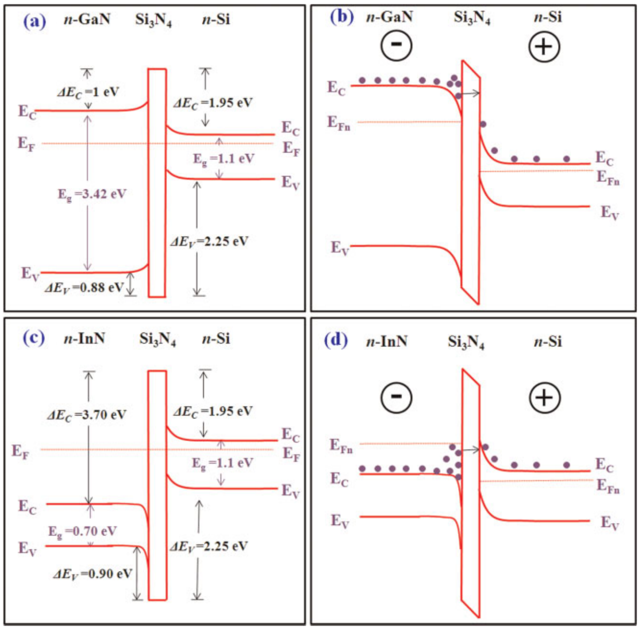

Figure 3 (online color at: www.pss-a.com) Energy-band diagrams of the (a) GaN/Si_3N_4/Si and (c) InN/Si_3N_4/Si isotype HJs under thermal equilibrium (b) and (d) under bias.

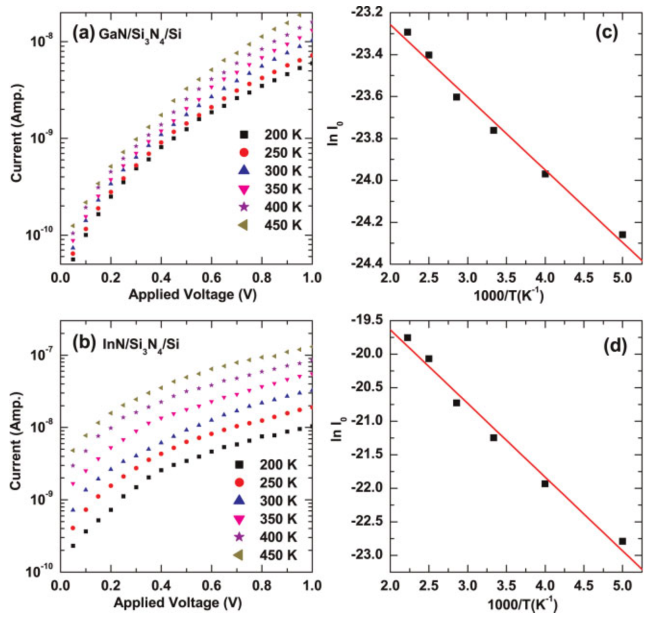

Figure 4 (online color at: www.pss-a.com) (a) and (b) Temperature dependence of the I–V characteristics of GaN/Si_3N_4/Si and InN/Si_3N_4/Si HJs. (c) and (d) Arrhenius plots of ln I_0 versus 1000/T of GaN/Si_3N_4/Si and InN/Si_3N_4/Si HJs, respectively. The pre-exponential factor I_0 has been obtained by extrapolating the forward current curves at 0 V.

and the Fermi level lies in the conduction band. Hence, the tunnelling barrier for electrons happens to be the same in the forward- and reverse-bias conditions, resulting in a symmetric nonlinear I–V behavior.

For further investigation of transport mechanisms, the log–log plots of the room-temperature forward-bias I–V data have been studied and are shown in Fig. 2c and d for sample (a) and (b), respectively. In sample (a), three distinct regions were observed depending on the applied voltage, which were assigned as region I, II, III. At low forward voltage (region I), the current transport follows a linear ohmic behavior ($I \propto V$) which is attributed to thermally generated carrier tunneling [12]. At a moderately higher junction voltage, the I–V characteristics follows a power law $I \propto V^{\eta}$, where $\eta = 2$ in region II and $\eta = 2.9$ in region III. In sample (b), only two distinct regions were observed I ($I \propto V$) and II ($I \propto V^{\eta}$, where $\eta = 1.9$). In the II and III regions, the current conduction is attributed to the space-charge-limited current (SCLC). The region I, for sample (b) is wider than that of sample (a), which could be caused by the presence of a large trap concentration in sample (b) compared to sample (a).

Figure 4a and b shows the temperature dependence of the I–V characteristics of GaN/Si_3N_4/Si and InN/Si_3N_4/Si HJs, respectively. At the lower voltage, the linearity of forward current can be clearly observed, which indicates that the current in this region is dominated by tunneling mechanism [13]. Therefore, the forward current can be explained by a multi-step tunneling model, which shows the dependence of current on both the temperatures and voltages [14]. According to this model, the forward current is given by the relation, $I_0 \propto \exp(-\Delta E_a/kT)$. In this relation, E_a is the activation energy of carrier conduction, k the Boltzmann constant, and T the absolute temperature. The pre-exponential factor I_0 can be obtained by extrapolating the forward current curves at 0 V. Figure 4c and d shows the Arrhenius plots of ln I_0 versus 1000/T with respect to the samples (a) and (b), respectively. As shown in the figure, ln I_0 satisfies a good linear relationship with $-1/T$ indicating a multi-step tunneling model [14]. The activation energies E_a estimated from this plot are about ~29 meV for GaN/Si_3N_4/Si and ~95 meV for InN/Si_3N_4/Si HJs.

4 Conclusions In conclusion, an ultrathin (~2.5 nm) Si_3N_4 layer was grown on Si (1 1 1) surface by exposing the surface to a radio-frequency nitrogen plasma and GaN/Si_3N_4/n-Si and InN/Si_3N_4/n-Si HJs were fabricated using PA-MBE. The HRXRD results establishing the epitaxial nature of GaN and InN thin-film highly oriented along the [0001] direction of the hexagonal wurtzite structure. The n-GaN/Si_3N_4/n-Si HJs show good rectifying behavior with an on/off ratio of 16 at 1.5 V, while n-InN/Si_3N_4/n-Si HJs show poor rectifying behavior with an on/off ratio of 1.5 at 1.5 V. The I–V characteristics of both HJs were discussed in terms of band diagram of HJs. In GaN/Si_3N_4/Si, HJs observed a lower trap concentration compared to InN/Si_3N_4/Si HJs. The dependence of forward currents on both the temperature and voltage were explained by using a multi-step tunneling model and the activation energies were estimated to be ~29 meV for GaN/Si_3N_4/Si and ~95 meV for InN/Si_3N_4/Si HJs.

References

[1] S. Nakamura, Science **281**, 956 (1998).
[2] C. J. Neufeld, N. G. Toledo, S. C. Cruz, M. Iza, S. P. DenBaars, and U. K. Mishra, Appl. Phys. Lett. **93**, 143502 (2008).
[3] H. W. Seo, L. W. Tu, Q. Y. Chen, C. Y. Ho, Y. T. Lin, K. L. Wu, D. J. Jang, D. P. Norman, and N. J. Ho, Appl. Phys. Lett. **96**, 101114 (2010).
[4] R. Averbeck and H. Riechert, Phys. Status Solidi A **176**, 301 (1999).
[5] T. Böttcher, S. Einfeldt, V. Kirchner, S. Figge, H. Heinke, D. Hommel, H. Selke, and P. L. Ryder, Appl. Phys. Lett. **73**, 3232 (1998).
[6] A. Dadgar, F. Schulze, M. Wienecke, A. Gadanecz, J. Blasing, P. Veit, T. Hempel, A. Diez, J. Christen, and A. Krost, N. J. Phys. **9**, 389 (2007).
[7] S. Sakai, T. Wang, Y. Morishima, and Y. Naoi, J. Cryst. Growth **221**, 334 (2000).
[8] M. Kumar, B. Roul, T. N. Bhat, M. K. Rajpalke, P. Misra, L. M. Kukreja, N. Sinha, A. T. Kalghatgi, and S. B. Krupanidhi, Mater. Res. Bull. **45**, 1581 (2010).
[9] M. Kumar, M. K. Rajpalke, T. N. Bhat, B. Roul, N. Sinha, A. T. Kalghatgi, and S. B. Krupanidhi, Mater. Lett. **65**, 1396 (2011).
[10] T. E. Cook, Jr., C. C. Fulton, W. J. Mecouch, R. F. Davis, G. Lucovsky, and R. J. Nemanich, J. Appl. Phys. **94**, 3949 (2003).
[11] W. Walukiewicz, J. W. Ager, III, K. M. Yu, Z. Liliental-Weber, J. Wu, S. X. Li, R. E. Jones, and J. D. Denlinge, J. Phys. D **39**, R83 (2006).
[12] S. Y. Liu, T. Chen, Y. L. Jiang, G. P. Ru, and X. P. Qu, J. Appl. Phys. **105**, 114504 (2009).
[13] J. D. Lee, C. Y. Park, H. S. Kim, J. J. Lee, and Y. G. Choo, J. Phys. D **43**, 365403 (2010).
[14] H. Matsuura, T. Okunu, H. Okushi, and K. Tanaka, J. Appl. Phys. **55**, 2656 (1984).

